New Method for Detection of Global Lightning Activity Using Schumann Resonance

Michał Dyrda[1,*], Andrzej Kułak[2,3], Janusz Młynarczyk[3], Michał Ostrowski[2], Jerzy Kubisz[2], Adam Michalec[2] and Zenon Nieckarz[4]

1. Institute of Nuclear Physics, Polish Academy of Sciences, ul. Radzikowskiego 152, Kraków, Poland
2. Astronomical Observatory, Jagiellonian University, ul. Orla 171, Kraków, Poland
3. AGH University of Science and Technology, Department of Electronics, al. Mickiewicza 30, 30-059 Kraków, Poland
4. Institute of Physics, Jagiellonian University, ul. Reymonta 4, 30-059 Kraków, Poland

ABSTRACT: In this paper we discuss a new method for a global lightning activity mapping using measurements of extremely low frequency (ELF) electromagnetic waves (EW) propagating in the Earth-ionosphere resonance cavity. With the data collected at the Hylaty ELF station, located in the Central Europe, we analyze the Schumann Resonances (SR) spectra with seven resonance peaks. The measurements are done quasi-continuously, using successive 10 minutes data intervals.

Kułak et al. [2006] found that the interaction of the standing and traveling waves leads to asymmetric shape of observed SR curves. Following this approach, we introduce a numerical model of the ELF electromagnetic waves propagation in the spherical Earth-ionosphere cavity and using this model we compute the asymmetric SR spectral templates for selected distances between the source and the observer. We fit the asymmetric curves describing seven SR maxima to the observational data and we calculate the distances to the thunderstorm centers by solving the inverse problem. As an example we investigate the lightning activity originating from the most intensive thunderstorm center in Africa. We use the observational radio data recorded in January and August 2011 and we construct the monthly lighting activity 1D maps using these data to study the differences in the location of the African storms centers during different seasons.

INTRODUCTION

Wilson, in 1920, proposed the hypothesis, that the global atmospheric electric circuit is driven by global lighting activity. Since that time, the research progress in this filed dramatically advanced. Nowadays, using different observational techniques from satellites for example the LIS detector [Christian et al. 2000], observing the Earth surface almost continuously, to the observations carried in the extremely

---

[*] Contact information: Michał Dyrda, Institute of Nuclear Physics PAS, Krakow, Poland, Email: Michal.Dyrda@ifj.edu.pl

low frequency (ELF) band it is possible to monitor the thunderstorm centers and the researchers are able to study the spatial and temporal variability of the lighting activity. These studies are very important in many fields, such as: physics of Earth ionosphere, the global climate variations and oscillations.

The Schumann resonance (SR), predicted by Schumann [1952], is believed to originate from electromagnetic emission, generated by the lightning activity in the Earth-ionosphere cavity. At ELF frequencies there is a very small attenuation, which allows electromagnetic waves to propagate even a few times around the globe before dissipating. Standing waves generate the constructive interference at *8, 14, 20, ...* Hz.

The first attempt to measure global lightning activity using the amplitude of the first Schumann resonance mode was done by Williams [1992]. He showed that there is a correlation between the mean temperature in the tropical rainforest regions and the diurnal mean amplitude of the first SR maximum.

Besides the ELF measurements, the ground based detection techniques of the global lightning activity, which measure the electromagnetic signals originating from discharges produced in the thunderstorms centers are connected to the radio observations in the very low frequency (VLF) band. There are quite a few such systems: the global ones for example WWLLN [Hutchins et al. 2011] and the local VLF monitoring systems for example LINET [Betz et al. 2004] and GLD360 [Pohjola and Makela 2013] in Europe.

In this paper we calculate the distances to the thunderstorm centers located in tropics by applying the SR power spectra templates computed for selected source-observer separations with the means of numerical modeling. Such approach is based on solution to the inverse problem and similar attempts were done previously by Heckamn et al. [1998] and Shvets [2001]. Our results are presented in the form of the 1D lightning activity map and as an illustration we present the results obtained for the lightning activity in Africa.

SPECTRAL LINES ASYMETRY IN DAMPED RESONATORS

Asymmetric spectral lines are observed in many resonant systems in Nature. Nevertheless, it is widely assumed that the damped oscillators spectra are described by symmetric Lorentz curves. Such point of view is based on classical theory of resonators in which the solutions of the wave equations are found using the method of separation variables. The classical solutions are restricted since they are based on a mathematical assumption that spatial field distribution does not depend on time. The damped resonator violates this condition because there are sources (lightning discharges) and hence the energy flows from sources to the resonant cavity. This leads to the dynamical field equilibrium and to describe such situation we have to use inhomogeneous wave equation. In such case, the field at each resonator's point is a superposition of the resonant field and the travelling waves. The superposition of both fields is responsible for the asymmetry of the observational resonant spectra and the resonant frequencies are functions of the distance [Kułak et al. 2006].

The height of the ionosphere is much smaller than the wavelength in the ELF band and the two dimensional (2D) resonator is a good model of the real three dimensional (3D) Earth-ionosphere cavity. The reduction of the 1D allows transforming the Maxwell field equations to the Kirchhoff equations

without losing any essential information about the propagations' mechanism. The 2D transmission line can approximate the Earth-ionosphere waveguide and hence the Two Dimensional Telegraph Equation (TDTE) can describe it [Madden, Thompson 1965]. The solutions of the TDTE can be obtained using numerical methods [Mushtak 1999] or by covering the sphere with a finite elements in the form of stripe lines [Kułak et al. 2003]. The models based on the transmission lines have an advantage, in contrast to the 3D models, in calculations efficiency and hence the possibility of carrying out numerical experiments. The asymmetry and changes of the resonant frequencies in observational ELF EW spectra are related to the interference of the resonant field and the traveling waves. To separate the components of these two fields we use the spectral decomposition method proposed by Kułak et al. [2006]. This method is based on the assumption that at any point of a resonator the power spectrum consists of a symmetric part (resonant component) and an asymmetric one (traveling wave component). In such case, the general form of spectrum at any point within a distance θ from a single source is given by equation [Kułak et al. 2006]:

$$W(f,\theta) = s + \frac{z}{f^m} + \sum_{k=1}^{N} \frac{a_k[1 + e_k(f - f_k)]}{(f - f_k)^2 + (\frac{g_k}{2})^2} \qquad (1),$$

where $W(f,\theta)$ is the ELF EW power spectrum, s represents the white noise term and it describes the local lightning discharges with flat spectra, a_k is the power of kth peak from the observed (in our case) $N = 7$ resonance peaks, e_k is the introduced asymmetry parameter, f_k – the peak frequency and g_k is the peak width. For a lack of asymmetry, $e_k = 0$, the shape of each peak becomes a respective Lorentzian curve and all parameters have their classical meanings. The color term z/f^m is used to describe the ELF station noise and any other external noises. The decomposition formula, given by equation (1) was found as the best approximation of the field equation in presences of sources existence and it was shown by Kułak et al. [2006] that such formula describes the observational ELF power spectra much better then the classical symmetric Lorentz curves. Also, the decomposition function, as defined by equation (1), reproduces the resonant frequencies f_k undistorted by traveling waves from nearby sources.

NUMERICAL MODEL SQ0005

In this section we construct physical and realistic model of the Earth-ionosphere cavity, which will be used in the computation of storms activity maps. This model is an extension of the model describing only three SR peaks, used in the paper by Kułak et al. [2006], to the model, that characterize seven SR modes. The physical parameters, used in the numerical solution of TDTE equation, i.e. damping coefficient, are taken form the above mentioned paper and our modeling is limited only to the magnetic field component since this component is measured by Hylaty ELF station. In this numerical model the resonance bands are suppressed in accordance with the theory of Legendre polynomials

The numerical solution of TDTE equation is obtained for a simple current impulse (the mathematical representation of such impulse current is the Dirac delta) and for *23* distances ranging from *23.6* degrees up to *156.4* degrees with the mean distance step around *5* degrees. Transforming this distances from degrees to kilometers, which is a more useful units for the readers, give the distances range from *2620* km

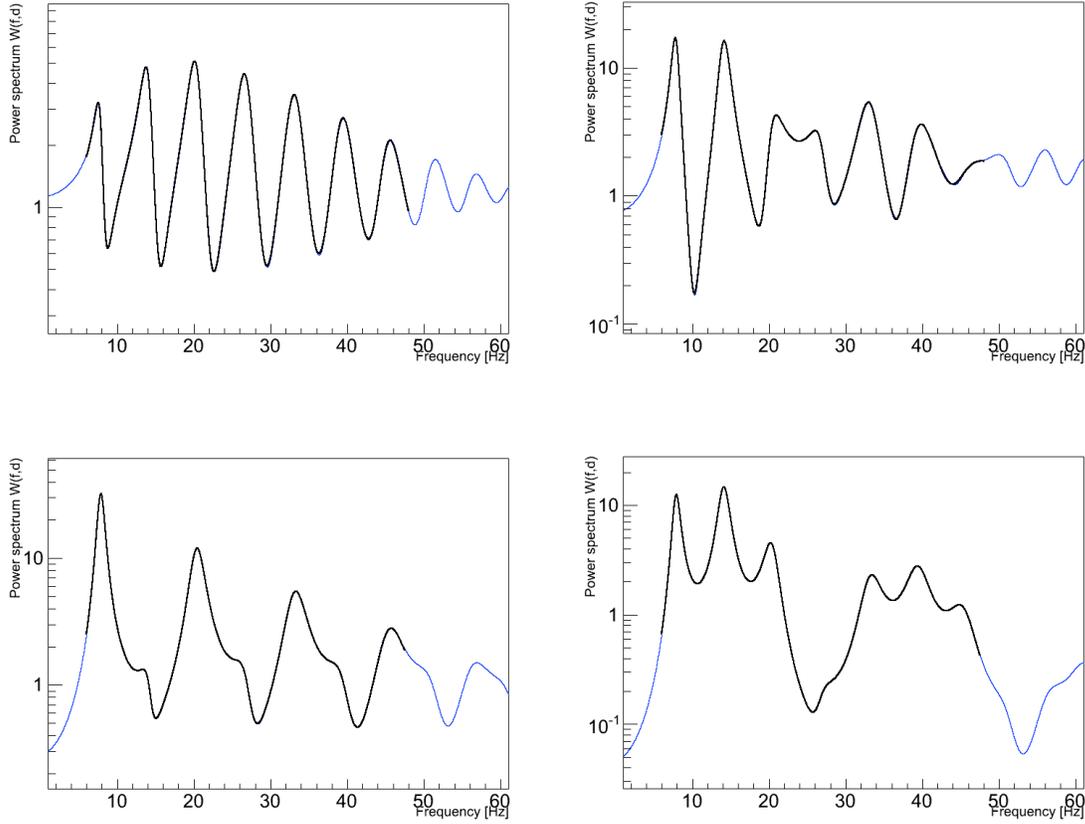to *17 394* km with a mean distance step about *550* km.

Figure 1: Numerical model data (in blue) and fitted asymmetric decomposition function (in black), given by equation (1) for selected source-observer separations: 2620 (23.6), 6672 (60), 10008 (90), 13344 (120) km (deg).

The decomposition function, given by equation (1) (with subtracted color term: z/f^{m}) is fitted to the numerical model data using the non-linear multiple least square algorithm in the frequency range: *4 – 48* Hz. The example of the numerical modeling, for four different source-observer separations, and the fitted decomposition function is shown in figure 1. The fitting procedure allows calculating the four parameters: a_k, e_k, f_k and g_k for seven resonant modes. In our modeling, as mentioned above, we do not include the color term z/f^{m}, but we keep the white noise term *s*, which is close to zero (within the statistical error) in all of the model cases since we do not include close discharges in numerical model *SQ0005*.
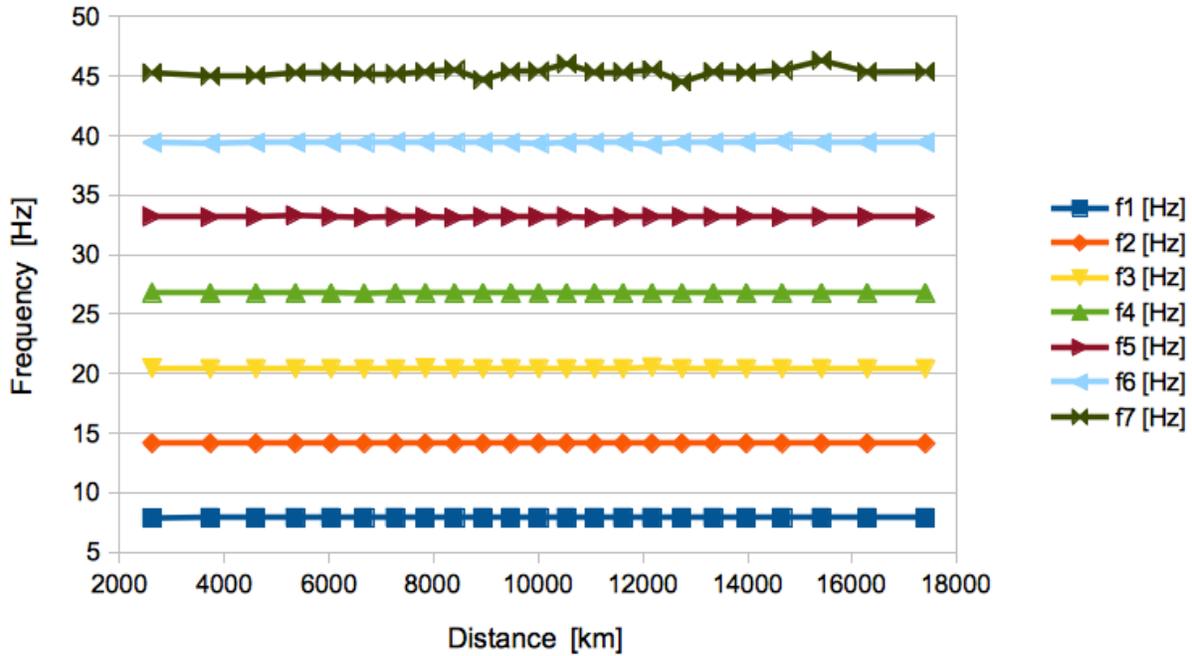
Figure 2: The frequencies of the seven SR mode as a function of the source-observer distance

Figure 2 shows the values of the peak frequencies for seven SR modes as a function of the source-observer separations. It is clearly visible that the frequencies do not depend on the distance to the source. Independence on the distance makes the frequencies f_k global values, which describe the physical state of resonant cavity in contrast to the Lorentzian (symmetric) frequencies, which are distance dependent.
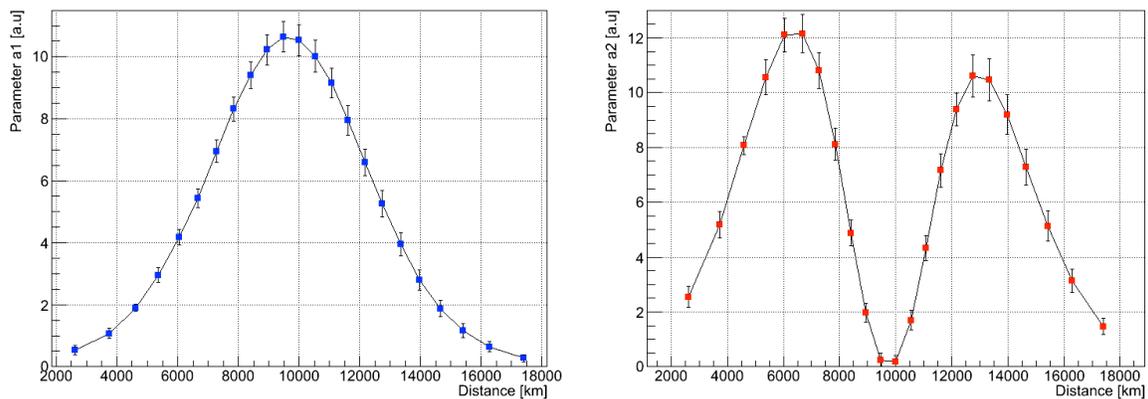

Figure 3: Amplitude of the first (left panel) and second (right panel) SR mode versus source-observer distance

The parameters a_k obtained from the decomposition of the numerical model *SQ0005*, as a function of the source-observer separations, for the first two SR mode are shown in figure 3. For the fundamental SR

mode at *8* Hz the parameter a_1 grows with the distance to the source and reaches the maximal value at the distance equal *10 008* km (*90* deg) and then it decreases with the source-observer separations. For the second SR mode there are two maxima and one minimum at θ = *10 008* km   (*90* deg), where this SR peak is suppressed. The same kinds of behavior are noted for the rest of SR modes, i.e. for the third SR peak there are *3* maxima and *2* minima. The parameters a_k depend on the source-observer separations and can be used in the calculations of the sources parameters.
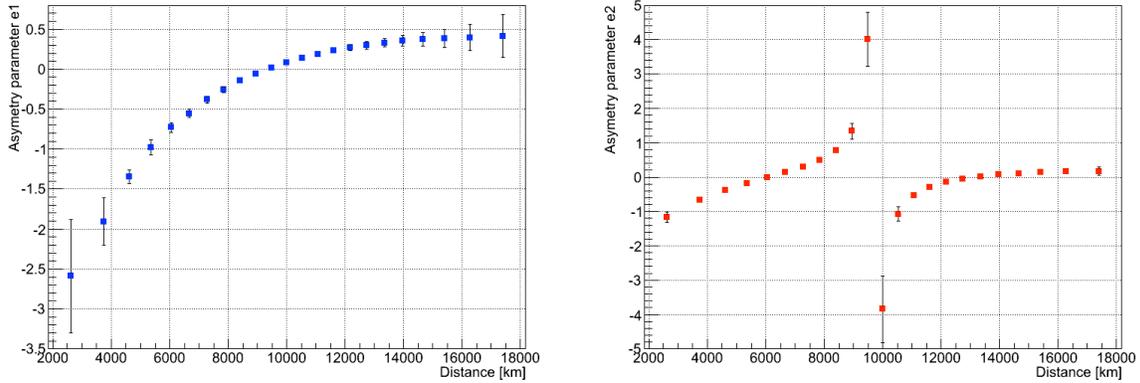

Figure 4: Distance dependencies of asymmetry parameters e_k for the first two SR modes. Please note that in some case the fitting (statistical only) error bars are smaller then the point size.

Asymmetry parameters e_k are related with the traveling wave field and similarly to power parameters a_k can provide information about the sources characteristics. The absolute values of asymmetry parameter e_1 are large near the sources and as a source-observer separation grows parameter e_1 tends toward zero. Figure 4 shows the dependence of the asymmetry parameters e_1 and e_2 on a distance between source and observer.   The asymmetry parameter e_1 is monotonic function of a distance θ and cloud be use to estimate the distance to the sources.

LEGENDRE POLYNOMIAL DECOMPOSITION AND CALCULATIONS OF THE STORMS ACTIVITIES MAPS

Our signal analysis procedure, based on Kułak et al. [2010], is performed separately for NS and EW antennas. However, in this work we make use of only one component (antenna) and thus we will obtain 1D maps. The analysis chain goes as follows. In the first step the transformation from time-domain to frequency-domain is done and the power spectrum is computed using the Fast Fourier Transform algorithm. The model function given by equation (1) is fitted to the observed power spectrum and it is done by non-linear multiple least square fitting procedure. As the results, parameters a_k, e_k, f_k and g_k are computed independently from two magnetic field components for each resonance peak. In the next step the vector **A** is constructed and the vector elements are a_k values. For each source with unit intensity and with the distance θ form the observer the theoretical values of amplitudes (b_k) for each peak are given by associated Legendre polynomials:

$$b_k(\theta) = \left(\frac{(2k\_1)}{\sqrt{k(k+1)}} P_k^1(\cos\theta) \right)^2 \qquad (2)$$

where θ source-observer distance is given in radians. Then the intensity vector $I(\theta)$, which describes the source intensity distribution as a function of distance θ is computed from the equation:

$$B \cdot I - A = \min \qquad (3),$$

where **B** is a matrix, which element are b_k – computed for chosen distances θ. The approach for construction of a map of global storms activity described in the steps above it is based on simple theoretical assumption, that intensities of lightning discharges are scaled using the associated Legendre polynomials. Another, a more realistic approach will be discussed in the next section.

COMPARISON BETWEEN OBSERVED AND MODELED SR POWER SPECTRA

The decomposition procedure gives 29 parameters for each power spectrum obtained using numerical model *SQ0005*. Then, the database of the numerical parameters for 7 SR modes is constructed, storing the parameters a_k, e_k, f_k and g_k. The term s - related to the white noise, which is essentially equal zero, is dismissed. The resulting database consists of 23 rows (one row for each modeled distance) and 29 columns - 28 that contain parameters fitted for a numerical solution plus one column providing the considered distance. In other words, each row in our data base contains parameters defining the asymmetric function denoted as $W_{th}^i(f)$, where the row number i gives the distance to the source.

The described database of the numerical parameters is used for construction of our 1-D storm activity map and hence the procedure applied for fitting the data is crucial. The initial steps in construction of a given map are the same as described in the previous section. The power spectrum is derived from the observational data using the FFT algorithm and the asymmetric function $W(f,\theta)$ given by equation (1) is fitted. Then the fitted white noise s and the term z/f^m are removed. The resulting derived asymmetric SR power spectrum function, which describes the real data, is denoted by $W_{obs}(f)$. In order to evaluate the distance from the source we look for a theoretical solution in the database, which best fits the observations. For each distance the chi-square test between the appropriate row in the database, which describes the function $W_{th}^i(f)$, and real data parameters for $W_{obs}(f)$ is performed to find the minimum. The chi-square value is calculated as follows:

$$\chi^2 = \int_1^{48} \frac{\left[W_{obs}(f) - I \cdot W_{th}^i(f) \right]^2}{I \cdot W_{th}^i(f)} df \qquad (4)$$

The smallest chi-square value yields the evaluated distance from the source and the respective storm intensity I is calculated, as given by the equation:

$$I = \frac{\int_{1}^{48} W_{obs}(f)df}{\int_{1}^{48} W_{th}^{i}(f)df} \qquad (5)$$

APPLICATION OF THE NUMERICAL MODEL SOLUTIONS TO THE OBSERVATIONAL DATA

The ELF Hylaty station is located in Poland (*49.19* N, *22.55* E) and it consists of two magnetic antennas [Kułak et al. 2014]. This location allows separating the storms activity from different regions of the world by independent measurement of two magnetic components B_{NS} and B_{EW}. The NS orientated antenna is able to measure the signals coming from lightning activity form Asian and American continent, whereas the EW antenna allows detecting storms activity of African center. It is worth stressing that this two antennas do not exclusively measure the mentioned storms centers, but both of them can detect the combination of signal from different regions, but main components of the measured signals are as referred above. Also, these centers appear mostly at different and specific parts of the day, which helps to discriminate the regions of the lightning activity origin. In this report we will focus on the lightning activity form the African center, which is easily detectable by the EW antenna and it peak activity is observed around 15 UTC [Chalmers, 1967].
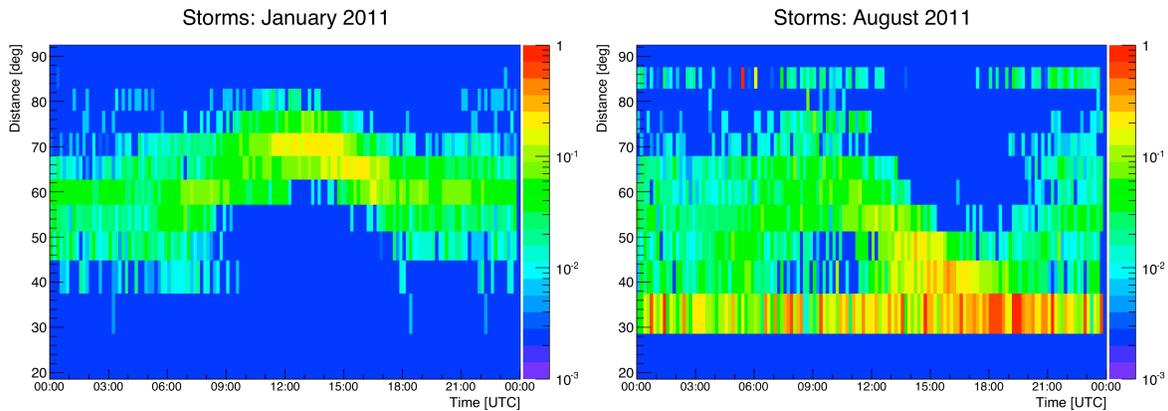

Figure 5: Cumulative daily storm intensities projected on the distance -- the UTC time plane. The distances to the storm centers were calculated using the numerical model *SQ0005*

In this section, the two-dimensional plots, our 1-D maps, will be used to show distances to, and intensities of the African storm centers as a function of the UTC time. Using the numerical model *SQ0005*, the storm activity was modeled with discrete distance steps ranging from *2620* km (*23* deg - the northern edge of the African continent) to around *10 000* km (*90* deg; behind the Cape Peninsula). The monthly cumulative storm activity maps obtained with our numerical fitting model (figure 5) were calculated as follows: for each *10* minute time interval the distance and lightning intensity were derived, and added to the respective map time-distance bin. The procedure was repeated for the entire month of

data. The color scales in the figure 5 show the cumulative monthly lightning intensities. The left panel in the figure presents the cumulative storm activity map for the considered winter data set, whereas the right panel for summer data set. The differences between these two maps can be clearly seen. In winter a major concentration of the lightning activity is visible for distances between *5600* and *8400* km (*50 - 75* deg) and time between *12* and *18* UTC. The late night and the early morning excesses are comparable with distances to the Asian storms activity center, whereas the evening excess in January data is comparable with distances to the American storm centers, but we were not able to remove these signals using data from only one magnetic antenna. In August, the most intense storms appear at distances between *3300* km (*30* deg) and *7800* km (*70* deg), times between the *12* and *20* UTC, but the major lightning activity is recorded in the range from approximately *3300* km (*30* deg) to *5500* km (*50* deg). A separate storm center formed at distances close to *9500* km (*85* deg) is detectable almost during the whole day. Thus the daily tracks of the African storm centers, depending on the season, are clearly visible at these two maps.
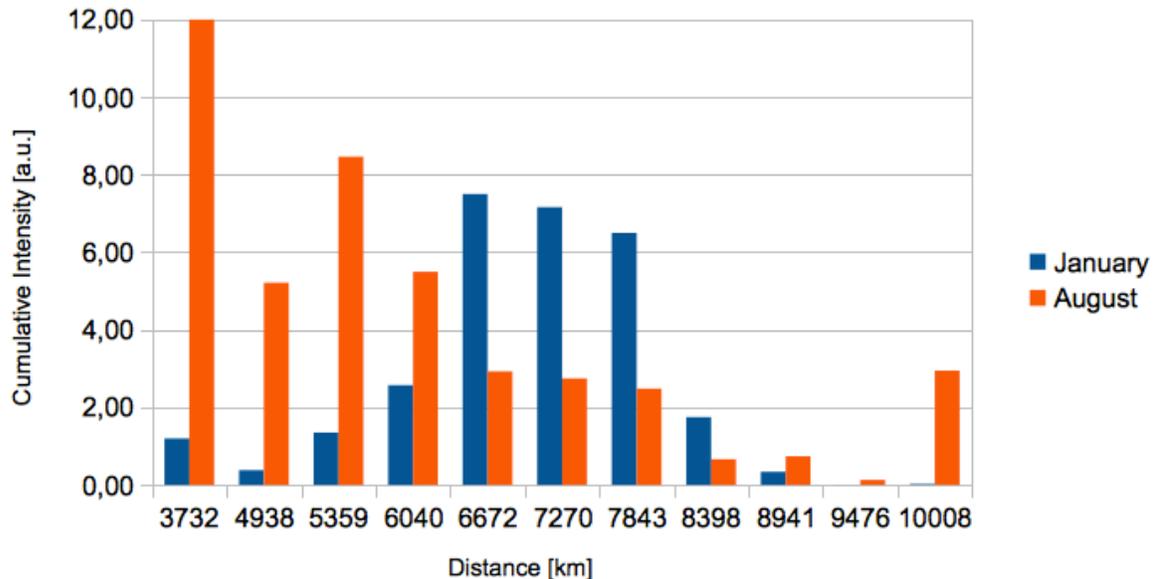

Figure 6: Distribution of the cumulative fitted intensities of storm centers for the two considered data sets, as a function of the storm distance.

Another comparison of the above cumulative storm activity maps is presented in the figure 6, where integrated lightning intensity as a function of distance was presented for both monthly data sets. The figure shows that in January most of the storm activity takes place at distances from about *5600* km (*50* deg), which is a distance between Hylaty station and the Equator, to *8400* km (*75* deg), with a peak value at the distance of ≈ *6672* km (*60* deg). The August storm activity pattern is substantially different from the January data. Then, a major lighting activity is observed at a distance of ≈ *3300* km (*30* deg). Then it decreases with a growing distance, to reach a (local) maximum at distances of the southern edge of the African continent. These results are in agreement with the cumulative monthly maps obtained from the

LIS measurements [LIS January map 2011, LIS August map 2011].

CONCLUSIONS

We presented a new method for detection of the global lighting activity using the SR measurements. We discuss the powerful method for SR spectra analysis based on the field decomposition in the spherical cavity, which allows for separations of the resonant field from the traveling waves contribution. Based on this method we present the construction of the 1D lightning activity maps using the theoretical approach with the associate Legendre polynomials. We introduce the numerical model *SQ0005* of the ELF EW propagation in the spherical Earth-ionosphere cavity and we use the decomposition method to compute the SR spectral templates for selected source-observer separations. Using the ELF data recorded in January and August 2011 we calculate the lightning activity maps applying the solutions to the inverse problem. We conclude that our approach gives the similar results as the monthly lightning activity maps obtained by the LIS detector. A new efficient method applying analytic modeling of the wave propagation to analyze the same problem is under elaboration now.

ACKNOWLEDGMENTS

REFERENCES

[1] Betz, H. D., Schmidt, K., Oettinger, P. and Wirz, M. (2004), Lightning detection with 3-D discrimination of intracloud and cloud-to-ground discharges, *Geophys. Res. Lett.*, **31**, 11108

[2] Chalmers, J. A. (1967), *Atmospheric Electricity*, Pergamon Press, New York

[3] Christian, H. J., Blakeslee, R. J. and Goodman, S. J. (2000), Lightning Imaging Sensor (LIS) for the International Space Station, *Space Technology and Applications International Forum*, **504**, 423

[4] Heckman, S. J., Williams, E. R. and Boldi, B. (1998), Total global lightning inferred from Schumann resonance measurements, *Journal of Geophysical Research*, **103**, 31775

[5] Hutchins, M. L., Holzworth, R. H., Rodger, C. J., Brundell, J. B. and McCarthy, M. (2011), Relative and Absolute Detection Efficiency of WWLLN, *AGU Fall Meeting Abstracts*, **A278**

[6] Kułak, A., Zięba, S., Micek, S., and Nieckarz, Z. (2003), Solar variations in extremely low frequency propagation parameters: 1. A two-dimensional telegraph equation (TDTE) model of ELF propagation and fundamental parameters of Schumann resonances, *Journal of Geophysical Research* (Space Physics), **108**, 1270

[7] Kułak, A., Młynarczyk, J., Zięba, S., Micek, S. and Nieckarz, Z. 2006: Studies of ELF propagation in the spherical shell cavity using a field decomposition method based on asymmetry of Schumann resonance curves. *Journal of Geophysical Research* (Space Physics), **111**, 10304

[8] Kułak, A., Kubisz J., Micek S., Michalec A, Nieckarz Z, Ostrowski M. and Zieba, S. (2010), Method and apparatus for monitoring storm activity on the Earth's surface in real time, *Patent US* 2010/0171485 **A1**

[9] Kułak, A., Kubisz, J., Michalec, A., Młynarczyk, J., Nieckarz, Z., Ostrowski, M. and Zięba, S. (2014), Hylaty Station for Extremely Low Frequency Electromagnetic Field Measurements, *Radio Science* (submitted)

[10] LIS January map, (2011), ftp://ghrc.nsstc.nasa.gov/pub/browse/lis/lis-summaries/2011/2011_january.png

[11] LIS August map, (2011), ftp://ghrc.nsstc.nasa.gov/pub/browse/lis/lis-summaries/2011/2011_august.png

[12] Madden, T. and Thompson, W. (1965), Low frequency electromagnetic oscillation of the Earth-ionosphere cavity, *Rev. Geophys.*, **3, 211**

[13] Mushtak, C., Boldi R. and Williams E. R. (1999), Schumann resonances and the temporal-spatial dynamics of global thunderstorm activity, *11th International Conference on Atmospheric Electricity*, 698

[14] Pohjola, H and Makela, A. (2013), The comparison of GLD360 and EUCLID lightning location systems in Europe, *Atmospheric Research*, **123**, 117

[15] Schumann, W.O. (1952), Über die strahlungslosen Eigenschwingen einer leitenden Kugel, die von einer Fuftschicht und einer Jonosphärenhülle umgeben ist, *Zeitschrift für Naturforsch.*, **7a**, 149

[16] Shvets, A. V. (2001), A technique for reconstruction of global lightning distance profile from background Schumann resonance signal, *Journal of Atmospheric and Solar-Terrestrial Physics*, **63**, 1061

[17] Williams, E. R. (1992), The Schumann Resonance: A Global Tropical Thermometer, *Science*, **256**, 1184